Applied Thermal Engineering 109 (2016) 958–969

Contents lists available at ScienceDirect

Applied Thermal Engineering

journal homepage: www.elsevier.com/locate/apthermeng

A review of high-temperature particle receivers for concentrating solar power

Clifford K. Ho

Sandia National Laboratories, United States

ARTICLE INFO

Article history:
Received 7 March 2016
Revised 17 April 2016
Accepted 21 April 2016
Available online 3 May 2016

Keywords:
Particle receiver
Concentrating solar power

ABSTRACT

High-temperature particle receivers can increase the operating temperature of concentrating solar power (CSP) systems, improving solar-to-electric efficiency and lowering costs. Unlike conventional receivers that employ fluid flowing through tubular receivers, falling particle receivers use solid particles that are heated directly as they fall through a beam of concentrated sunlight, with particle temperatures capable of reaching 1000 °C and higher. Once heated, the hot particles may be stored and used to generate electricity in a power cycle or to create process heat. Because the solar energy is directly absorbed by the particles, the flux and temperature limitations associated with tubular central receivers are mitigated, allowing for greater concentration ratios and thermal efficiencies. Alternative particle receiver designs include free-falling, obstructed flow, centrifugal, flow in tubes with or without fluidization, multi-pass recirculation, north- or south-facing, and face-down configurations. This paper provides a review of these alternative designs, along with benefits, technical challenges, and costs.

Contents

1. Introduction

Higher efficiency power cycles are being pursued to reduce the levelized cost of energy from concentrating solar power tower technologies [1]. These cycles, which include combined air-Brayton, supercritical-CO_2 (sCO_2) Brayton, and ultra-supercritical steam cycles, require higher temperatures than those previously achieved using central receivers. Current central receiver technologies employ either water/steam or molten nitrate salt as the heat-transfer fluid in subcritical Rankine power cycles. The gross

E-mail address: ckho@sandia.gov

http://dx.doi.org/10.1016/j.applthermaleng.2016.04.103
1359-4311/

thermal-to-electric efficiency of these cycles in currently operating power-tower plants is typically between 30% and 40% at turbine inlet temperatures < 600 °C. At higher input temperatures, the thermal-to-electric efficiency of the power cycles increases. However, at temperatures greater than 600 °C, molten nitrate salt becomes chemically unstable, producing oxide ions that are highly corrosive [2], which results in significant mass loss [3].

Technical challenges and requirements associated with high-temperature receivers include the development and use of geometric shapes (e.g., dimensions, configurations), materials, heat-transfer fluids, and processes that maximize solar irradiance and absorptance, minimize heat loss, and have high reliability at high temperatures over thousands of thermal cycles [4]. Advantages of direct heating of the working fluid include reduced exergetic losses through intermediate heat exchange, while advantages of indirect heating include the ability to store the heat-transfer media (e.g., molten salt, solid particles) for energy production during non-solar hours.

Ho and Iverson [4] showed that a high solar concentration ratio on the receiver and reduced radiation losses are critical to maintain high thermal efficiencies at temperatures above 650 °C. Reducing the convective heat loss is less significant, although it can yield a several percentage point increase in thermal efficiency at high temperatures (note that the convective heat loss in cavity receivers can be a factor of two or more greater than that in external receivers because of the larger absorber area [5]). Increasing the solar absorptance, α, and/or decreasing the thermal emittance, ε, can also increase the thermal efficiency.

Particle receivers are currently being designed and tested as a means to achieve higher operating temperatures (>700 °C), inexpensive direct storage, and higher receiver efficiencies for concentrating solar power technologies, thermochemical reactions, and process heat [6–23]. Unlike conventional receivers that employ fluid flowing through tubular receivers, particle receivers use solid particles that are heated—either directly or indirectly—as they fall through a beam of concentrated sunlight. Once heated, the particles may be stored in an insulated tank and used to heat a secondary working fluid (e.g., steam, CO_2, air) for the power cycle (Fig. 1). Particle receivers have the potential to increase the maximum temperature of the heat-transfer media to over 1000 °C. Thermal energy storage costs can be significantly reduced by directly storing heat at higher temperatures in a relatively inexpensive medium (i.e., sand-like particles). Because the solar energy is directly absorbed in the particles, the flux limitations associated with tubular central receivers (high stresses resulting from the containment of high temperature, high pressure fluids) are significantly relaxed. The falling particle receiver appears well-suited for scalability ranging from 10 to 100 MW_e power-tower systems.

Previous studies have considered alternative particle receiver designs including free-falling [18], obstructed flow [24,25], centrifugal [20,21,26,27], flow in tubes with or without fluidization [15,22,23,28–31], multi-pass recirculation [9,17] north- or south-facing [6,11], and face-down configurations [32]. In general, these particle receivers can be categorized as either direct or indirect particle heating receivers. Direct particle heating receivers irradiate the particles directly as they fall through a receiver, while indirect particle heating receivers utilize tubes or other enclosures to convey and heat the particles. The following section summarizes both direct and indirect particle heating receivers and presents advantages and challenges associated with each.

2. Particle receiver designs

2.1. Direct particle heating receivers

2.1.1. Free-falling particle receivers

The most basic form of a direct particle heating receiver consists of particles falling through a cavity receiver, where the particles are irradiated directly by concentrated sunlight. The particles are released through a slot at the base of a hopper above the receiver, producing a thin sheet (or curtain) of particles falling through the receiver (Fig. 2).

A number of assessments and studies have been performed on direct free-falling particle receivers since its inception in the 1980s [6–10,12–14,17–19,33–48]. In 2010, Tan and Chen provided an overview of the prior research on free-falling particle receivers [19]. The majority of those studies focused on modeling the particle hydraulics and radiant heat transfer to falling particles. Various geometries and configurations of falling particle receivers have been considered, including north/south facing cavity receivers as well as face-down cavity receivers with a surrounding heliostat field [8,32,42]. In 2008, Siegel et al. performed one of the first on-sun tests (in batch mode) of a simple free-falling particle receiver [18,49]. Those tests achieved ~50% thermal efficiency, and the maximum particle temperature increase was ~250 °C.

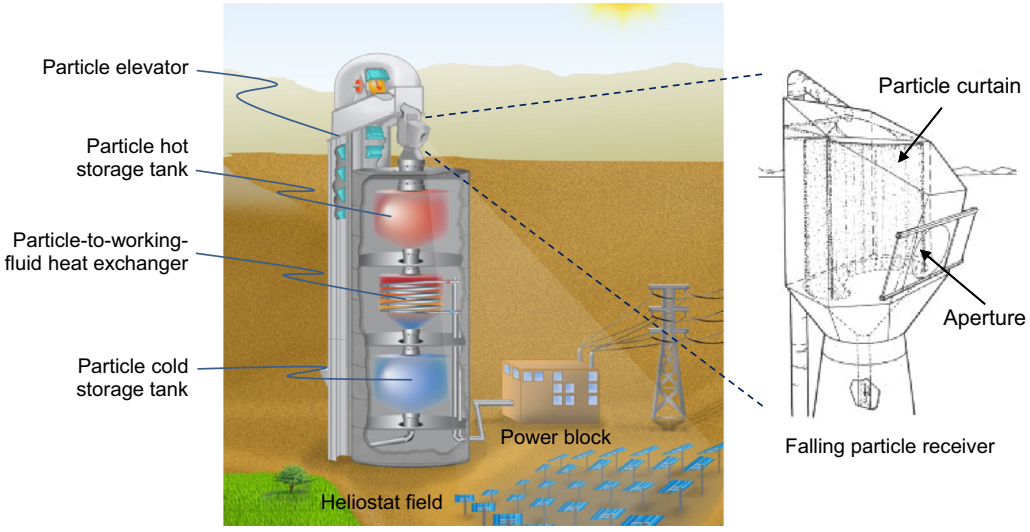

Fig. 1. Falling particle receiver system with integrated storage and heat exchange [9].

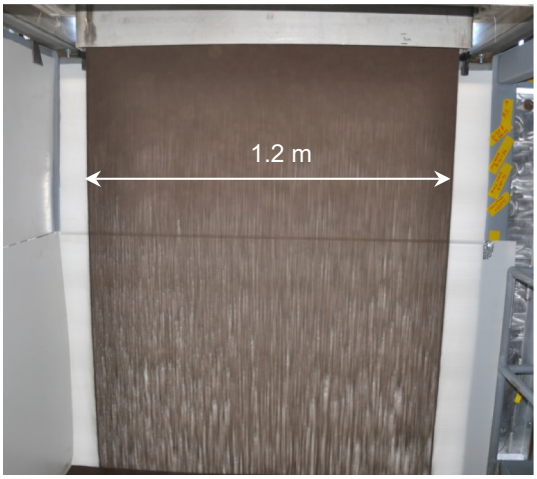

Fig. 2. Falling particle curtain released through 1.2 m × 11.1 mm discharge slot aperture [33].

More recently, Ho et al. have performed on-sun tests of a 1 MW_{th} continuously recirculating particle receiver with bulk particle outlet temperatures reaching over 700 °C, and thermal efficiencies from ~50% to 80% [24,25] (Fig. 3). Results showed that the particle temperature rise and thermal efficiency were dependent on particle mass flow rate and irradiance. Higher particle mass flow rates yielded greater thermal efficiencies but lower particle temperature rise. As the particle mass flow rate increased (by increasing the particle discharge slot aperture size), the solids volume fraction increased and the particle curtain became more opaque. Thus, while more sunlight was intercepted and absorbed by the curtain for a greater thermal efficiency, additional shading and blocking reduced the bulk outlet temperature of the particles for a given irradiance. At higher irradiances of 1000 suns and higher, a greater amount of energy is absorbed by the particles for a given receiver size with relatively less heat loss than for lower irradiances. Technical challenges that were identified during the tests included non-uniform irradiance distributions on the particle curtain, variable mass flow rates, wind impacts, particle loss through the aperture, particle elevator reliability, and wear on the receiver walls from direct flux and high temperatures (>1000 °C).

The heat gain and exit temperature of particles falling through concentrated sunlight depends on the particle mass flow and amount of time spent in the heated region of the receiver. Increasing this residence time is a critical aspect in achieving desired high temperatures. One way to increase the residence time is to recirculate the particles through the receiver multiple times, increasing in temperature over each successive drop [6,32,41]. Although particle recirculation is an attractive means to increase particle heating, additional particle elevators or conveyance systems would be required, which would increase complexity and cost. Previous studies have modeled recirculating particle flow through the receiver, but prototypes have not yet been demonstrated.

Kim et al. [13] performed tests of particles free-falling along a 3 m drop length to evaluate the influence of wind direction (induced by fans). They found that the most particles were lost through the aperture when the wind was parallel to the aperture and when the cavity depth was shallow. The least amount of particle loss occurred when the wind was oriented directly toward (normal to) the aperture. Air recirculation and air curtains have been proposed as a means to mitigate the impacts of wind on particle flow and to reduce convective losses [19,43,45,50–53]. Tan et al. [19,51–53] simulated the use of an aerowindow (transparent gas stream along the aperture) to mitigate heat loss and wind impacts in falling particle receivers (Fig. 4). Tan et al. [53] found that aerowindows could reduce the heat loss by up to 10% depending on external wind direction and speed. However, no tests or validation studies were performed, and few parametric analyses have been conducted to evaluate important air-recirculation parameters. Ho et al. [43,45] performed experimental and numerical studies that evaluated the impact of an air curtain on the performance of a falling particle receiver. Unheated experimental studies were performed to evaluate the impact of various factors (particle size, particle mass flow rate, particle release location, air-curtain flow rate, and external wind) on particle flow, stability, and loss through the aperture (Fig. 4). Numerical simulations were performed to evaluate the impact of an air curtain on the thermal efficiency of a falling particle receiver at different operating temperatures. Results showed that the air curtain reduced particle loss when particles were released near the aperture in the presence of external wind, but the presence of the air curtain did not generally improve the flow characteristics and loss of the particles for other scenarios. Larger particles and mass flow rates were also shown to reduce particle loss through the aperture. Numerical results showed that the presence of an air curtain could reduce the convective heat losses, but only at higher temperatures (>600 °C) when buoyant hot air leaving the aperture was significant.

2.1.2. Obstructed particle receivers

Another method to increase the residence time of particles within the concentrated sunlight is to obstruct the flow with porous structures or an array of obstacles that mechanically impede their descent and slow the downward velocity while still allowing direct absorption of concentrated solar energy. Early concepts of obstructed flow designs were introduced by Sandia in the 1980s by using ceramic structures suspended from the back wall to decelerate the particles [35]. No analytical or experimental studies

Fig. 3. On-sun testing of a falling particle receiver at the National Solar Thermal Test Facility at Sandia National Laboratories, Albuquerque, NM.

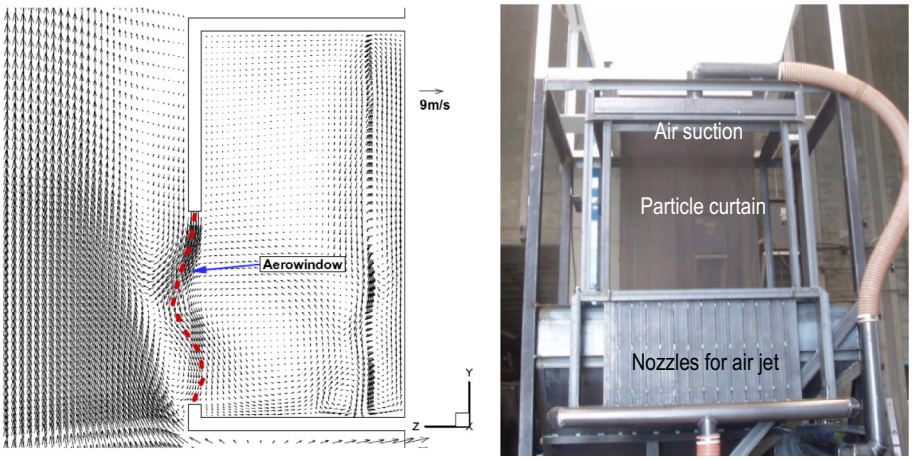

Fig. 4. Left: Air curtain modeling for particle receivers [53]. Right: Experimental system to test air curtains for particle receivers [45].

were published, however. More recently, King Saud University and the Georgia Institute of Technology investigated the use of interconnected porous structures (metallic or ceramic foam blocks) to slow the flow of particles [54].

Additional studies evaluated the use of a staggered array of porous mesh structures [9,55] to impede the flow of particles for increased residence time. In 2015, Ho et al. performed on-sun tests of a particle receiver consisting of a staggered array of stainless-steel chevron-shaped mesh structures [25] (Fig. 5). Peak particle temperatures reached over 700 °C near the center of the receiver, but the particle temperature increase near the sides was lower due to a non-uniform irradiance distribution. At a particle inlet temperature of ~440 °C, the particle temperature increase was nearly 30 °C per meter of drop length, and the thermal efficiency was ~60% for an average irradiance of 110 kW/m^2. At an average irradiance of 211 kW/m^2, the particle temperature increase was ~60 °C per meter of drop length, and the thermal efficiency was ~65%. While the obstructed-flow design seemed to improve the particle heating and reduce the impacts of wind and particle loss through the aperture, there were problems with the stainless steel 316 mesh materials overheating, oxidizing, and deteriorating as a result of direct irradiance from the concentrated sunlight and wear from the particles. New materials and operational strategies are being investigated to mitigate mesh deterioration.

Another obstructed flow design employs a spiral ramp along which particles flow under the influence of gravity and mechanically induced vibration [56]. Models and tests were performed that demonstrated that the particles could reach 650 °C at the outlet after 30 min of radiant power of 5 kW at the aperture. The measured thermal efficiency was ~60%. This design, however, requires beam-down optics, and a significant amount of particle flow may be challenging with this design.

A final obstructed flow design that employs beam-down optics lifts the particles upward with a screw elevator toward an aperture. The particles are irradiated by concentrated sunlight before spilling into the hollow screw for subsequent heat exchange and reaction. This particle receiver design was developed as part of a thermochemical reactor to reduce particles that are subsequently oxidized to produce either hydrogen or carbon monoxide [57]. Fig. 6 shows a schematic of the receiver reactor, which also takes advantage of preheating and recuperation since the heated particles that fall through the hollow screw also preheat the oxidized particles being lifted up along the flights of the screw. While analyses have been performed to evaluate the performance and efficiency [58,59], prototype have not yet been tested.

2.1.3. Rotating kiln/centrifugal receivers

Rotating kilns were proposed as early as 1980 for use in solar particle heating applications [22]. The general principle is to feed particles into a rotating kiln/receiver with an aperture at one end of the receiver to allow incoming concentrated sunlight. The centrifugal force of the rotating receiver causes the particles to move along the walls of the receiver while they are irradiated by the concentrated sunlight. Early tests by Flamant et al. showed that these systems have a very high absorption factor (0.9–1), but the thermal efficiency was low (10–30%) for heating of $CaCo_3$ at particle mass flow rates of ~1 g/s. More recently, Wu et al. [20,21,26,27] developed a centrifugal particle receiver design and prototype that employs a similar concept (Fig. 7). Small bauxite ceramic particles (~1 mm) were introduced into a rotating centrifugal receiver with different inclination angles at mass flow rates of ~3 to 10 g/s. The particles were irradiated using a 15 kW$_{th}$ solar simulator with an irradiance ranging from ~300 to 700 kW/m^2. For a face-down receiver inclination and incident irradiance of 670 kW/m^2, Wu

Fig. 5. Images of particle flow over a staggered array of chevron-shaped mesh structures.

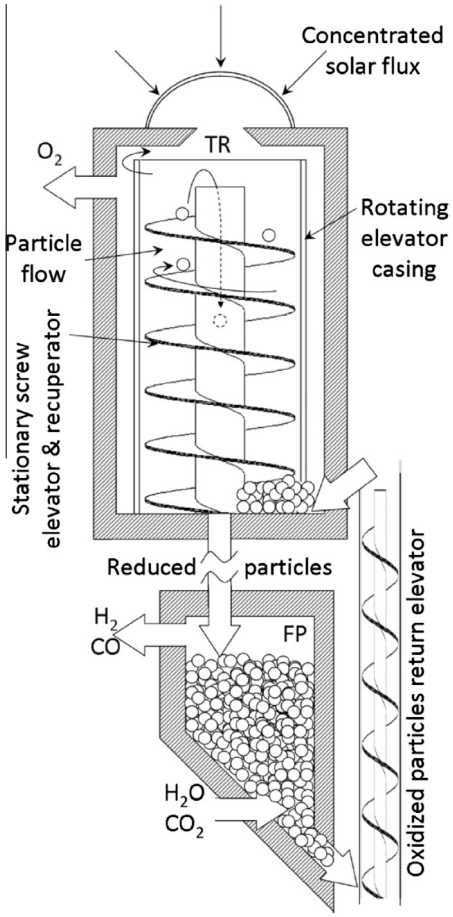

Fig. 6. Schematic of a moving packed bed particle reactor [57].

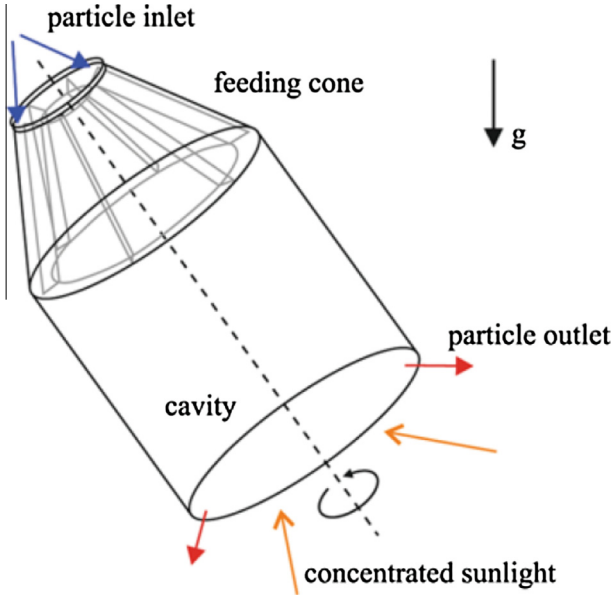

Fig. 7. Schematic of a rotary kiln/centrifugal receiver [27].

et al. reported a particle outlet temperature of 900 °C and a receiver efficiency of about 75% (±4%) [20]. Challenges include maintaining a constant and sufficient mass flow rate of particles at larger scales, parasitic energy requirements, and reliability associated with a large rotating receiver system.

2.1.4. Fluidized particle receivers

Fluidization of solid particles in a solar receiver have been proposed for several decades, beginning in the late 1970s and early 1980s by Flamant et al. for thermochemical processing and heating [22,23] and by Sandia for power production [7]. Flamant et al. [22,23] tested a fluidized-bed receiver that consisted of a vertical transparent silica tube (15 cm long × 6.5 cm diameter) that was fluidized with compressed air from the bottom and irradiated at the top. Particles that were tested included zirconia, silica sand, chamotte, and silicon carbide. For a mean flux density of ~500 kW/m^2, the measured equilibrium temperature of the particles ranged from ~1200 K for silica sand to over 1400 K for silicon carbide particles. Thermal efficiencies were reported between 0.2 and 0.4 [23]. The ability to convey the particles and achieve adequate mass flow rates (for power production or continuous processes) may pose a challenge.

More recently, researchers at the Chinese Academy of Sciences [60–62] have performed numerical and experimental studies on the thermal performance of an air receiver with silicon carbide particles in transparent quartz tubes. Air is blown upward through the particles in the quartz tubes while the tubes and particles are irradiated with concentrated sunlight from a 10 kW_{th} furnace (Fig. 8). Results of those tests showed that the heated air reached over 600 °C with minimum temperature differences between the particles and the air below 10 °C, indicating good heat transfer between the air and the particles.

Steinfeld et al. [31] designed and tested a fluidized bed receiver reactor that employed a vortical flow of air in a conical-shaped receiver. The particle/gas stream was introduced near the aperture, where concentrated sunlight entered the receiver and heated the swirling particles before the particles exited the receiver. The prototype reactor was tested to evaluate the thermal decomposition of calcium carbonate at 1300 K. The mean thermal absorption efficiency was 43% with a peak flux of ~1400 kW/m^2 at the aperture.

A final type of fluidized particle receiver involves the use of very small carbon particles dispersed in air that flows through the receiver. Concentrated sunlight irradiates and oxidizes the carbon particles, which volumetrically heats pressurized air passing through the receiver for high-temperature Brayton cycles. Abdelrahman et al. [63] and Hunt [64] first introduced this concept in 1979, and Hunt and Brown [65] performed tests on a prototype receiver that heated the air to 1000 K. Miller and Koenigsdorff [66,67] developed theoretical analyses and thermal modeling of the small particle solar receiver. Additional modeling and design optimization of the small particle heating receiver were performed in recent years as well [68–71]. Potential advantages include the following: solar radiation is absorbed throughout the gas volume due to the large cumulative surface area of the particles; higher incident fluxes with no solid absorber that can be damaged; particles are oxidized leaving a particle free outlet stream [66]. Challenges include the development of a suitable window for the pressurized receiver and the development of a solid–gas suspension system that maintains a uniform particle concentration and temperature within the receiver.

2.2. Indirect particle heating receivers

2.2.1. Gravity-driven particle flow through enclosures

Ma et al. [15,30,72] proposed an indirectly heated particle receiver with particles flowing downward under the force of gravity around a staggered array of tubes within an enclosure. The tubes were irradiated by concentrated sunlight on the interior surfaces

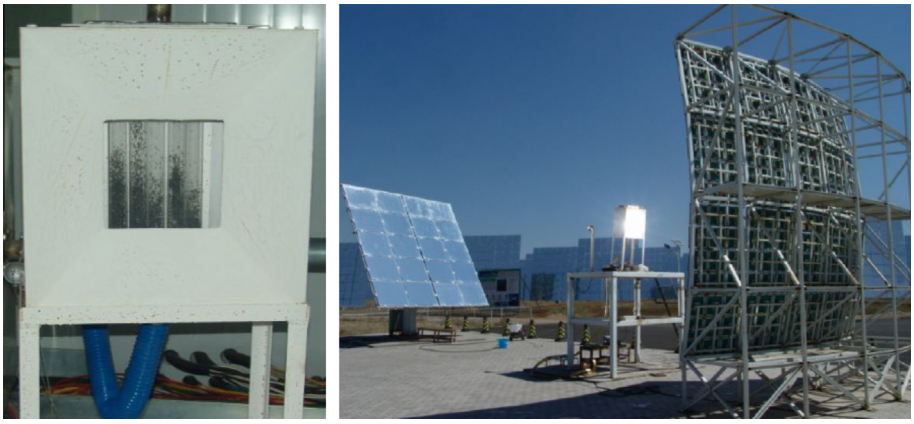

Fig. 8. Images of testing of a quartz-tube particle air receiver [60].

while transferring heat to the particles flowing around the exterior side of the tubes inside of an enclosure (Fig. 9). Small-scale tests and models were performed that showed that the heat transfer to the particles was limited in locations around the tubular structures where the particles lost contact with the heated wall surfaces. Specific data on particle temperatures and thermal efficiencies were not available, and no on-sun tests have been performed. Other limitations included maintaining a sufficient mass flow and obtaining a significant penetration and uniform flux of concentrated sunlight within the tubular cavities. Advantages to this design include no loss of particles through an open aperture and reduced heat losses relative to an open cavity receiver.

2.2.2. Fluidized particle flow through tubes

Flamant et al. [28,29,73] have proposed and demonstrated an indirect particle receiver in which the particles are forced upward through irradiated tubes by airflow, which fluidizes the particles and increases heat transfer from the tube walls to the flowing particles. Particle temperature increases of greater than 200 °C were recorded in a 50 cm long stainless steel AISI 304L tube with irradiances ranging from ~200 to 400 W/m^2. Suspension temperatures at the outlet of the irradiated tubed were up to 750 °C, and the wall-to-suspension heat transfer coefficient was determined to be 420–1100 W/m^2 K for solid mass fluxes of 10–45 kg/m^2 s, respectively. Thermal efficiencies were not reported. Challenges in this system include parasitic energy requirements to fluidize the particles through the receiver tubes with sufficient mass flow to meet desired power requirements. The potential for hot spots and significant tube surface temperatures that radiate energy to the environment also exist.

2.3. Summary of particle receiver technologies

Table 1 summarizes the different types of direct and indirect particle receiver designs. The achievable outlet temperature and thermal efficiency is reported if data were available. The benefits and challenges of each design is also presented, along with relevant references. Table 2 presents a summary of performance and cost comparisons between the falling particle receiver and other conventional solar thermal receivers. Overall, each of the particle receiver designs have promising advantages, along with challenges that need to be addressed. Directly heated particle receivers have a significant advantage of direct particle heating, but particle loss may be a problem in open cavities with significant wind effects. Indirect particle receivers have the advantage of particle containment and no particle losses, but additional heat transfer resistance between the irradiated surface and the particles is a challenge. Fluidizing the particles within tubes has been shown to enhance

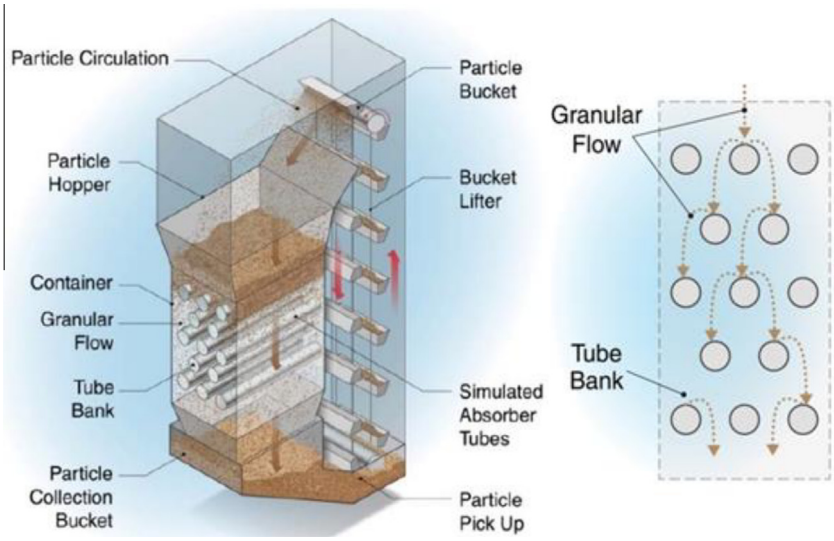

Fig. 9. Indirect particle receiver with particles flowing inside an enclosure around tubes whose interior surfaces are exposed to concentrated sunlight [30].

Table 1
Summary of particle receiver designs.

Receiver design	Outlet temperature/thermal efficiency	Benefits	Challenges/research needs	References
Direct particle receivers				
Free-falling	>700 °C/ ~50% to 80%	Capable of achieving high temperatures, direct irradiance of particles reduces flux limitations (on tubular receivers), particles can be stored at high temperatures, particles can be cheaper than molten salt	Need lower radiative and convective heat losses, higher concentration ratios, lower particle attrition, greater solar absorptance, lower thermal emittance, increased particle residence time, more effective particle/fluid heat exchangers	[7,10,14,18,19,24,32,35,41,49,51–53,74–77]
Obstructed	>700 °C/ ~60% to 90%	Capable of achieving high temperatures, obstructions slow particle flow and increase residence time, flow is more stable than free-fall, less particle loss	Hot spots and continuous flow over obstructions may cause deterioration or failure if mass flow and cooling is not maintained; additional cost of fabricating obstructions	[24,25,54,78]
Rotating kiln/centrifugal	900 °C/75%	High particle temperatures, control of residence time via rotational speed of receiver	Maintaining a constant and sufficient mass flow rate of particles at larger scales, parasitic energy requirements, and reliability associated with a large rotating receiver system	[20,21,26,27]
Fluidized-bed	>1000 °C/20–40%	Excellent heat transfer to fluidized particles with increased residence time	Parasitic energy requirements to fluidize particles, maintaining sufficient mass flow for desired power requirements	[22,23,31,60–62]
Indirect particle receivers				
Gravity-driven flow in enclosures	No data available	High particle temperatures theoretically achievable; no particle loss due to containment	Additional heat transfer resistance from irradiated walls to particles; hot spots on enclosures may cause deterioration or failure if mass flow and cooling is not maintained	[15,30,72]
Fluidized flow in tubes	750 °C/thermal efficiency not reported	Enhanced heat transfer from walls to particles due to fluidization; no particle loss due to containment	Parasitic energy requirements to fluidize particles; maintaining sufficient mass flow for desired power requirements; hot spots on enclosures may cause deterioration or failure if mass flow and cooling is not maintained	[28,29,73]

Table 2
Comparison of particle receiver to other solar thermal receiver technologies.

	Solar thermal receiver technology					References
	Falling particle receiver	Steam receiver	Molten nitrate salt receiver	Liquid sodium receiver	Volumetric air receiver	
Direct energy storage (> 6 h)?	Yes	No	Yes	No	No	
Maximum irradiance (kW/m^2)	Unlimited (>2000)	600	600	1500–2500	900	[7,79]
Maximum temperature (°C)	>1000 °C up to melting point of particles (2000 °C)	650 °C	<600 °C	800 °C	800–900 °C	[7,79]
Thermal efficiency (%)	50–90%	80–90%	80–90%	90–96%	50–80%	[4,24,80]
Cost ($/kW$_t$)	125	~140 to 200	~140 to 200	140–200	No data	Section 4, [1]
Restrictions/limitations	N/A	High pressure steam requires thicker tubing and more expensive materials	Salt freezes at 200 °C; requires trace heating	Sodium reacts violently with water and spontaneously ignites in air above 115 °C	N/A	

the heat transfer. For large-scale electricity production, which will require significant particle mass flow rates, gravity-driven flow (free-falling or with obstructions) appear to be the most promising.

3. Particles

A variety of ceramic and silica-based particles have been investigated for high-temperature falling particle receivers. Commercially available ceramic particles that are used for hydraulic fracturing are well-suited for falling particle receivers because of their durability, high solar absorptance, and low cost. Ceramic particles appear best suited for direct-heating particle receivers to absorb as much concentrated sunlight as possible. Table 3 shows the optical properties of several different particles. Spherical sintered-bauxite particles have high solar absorptance (>0.9) and resistance to abrasion and sintering at high temperatures and pressures [46,48,81]. Tests were performed that exposed the particles to high temperatures (up to 1000 °C) while falling through an hour-glass-like apparatus that rotated 180° continuously over thousands of cycles. Results indicated that the ceramic particles did not show significant signs of wear or sintering [46]. Regarding the solar absorptance, continuous heating of the sintered bauxite particles in air over 700 °C for 500 h showed that the solar absorptance degraded by just one or two percentage points from oxidation, but appeared to stabilize [48]. Further testing showed that the particle solar absorptance could be rejuvenated through thermal or chemical reduction [48].

Silica-based particles (i.e., sand) are inexpensive and abundant, but they lack high solar absorptance, and some sands (Olivine) can

Table 3
Optical properties for several different particles and Pyromark 2500 as a baseline.

Material name	Type	Solar weighted absorptivity (–)	Thermal emissivity (–)[a]	Selective absorber efficiency (–)[b]
Carbo HSP	Sintered bauxite	0.934	0.843	0.864
CarboProp 40/70	Sintered bauxite	0.929	0.803	0.862
CarboProp 30/60	Sintered bauxite	0.894	0.752	0.831
Accucast ID50K	Sintered bauxite	0.906	0.754	0.843
Accucast ID70K	Sintered bauxite	0.909	0.789	0.843
Fracking Sand	Silica	0.55	0.715	0.490
Pyromark 2500	Commercial paint	0.97	0.88	0.897

[a] Spectral directional reflectance values were measured at room temperature. The total hemispherical emissivity was calculated assuming a surface temperature of 700 °C.
[b] Q is assumed to be 6×10^5 W/m^2 and T is assumed to be 700 °C (973 K): $\eta_{sel} = \frac{\alpha_s Q - \varepsilon \sigma T^4}{Q}$.

Table 4
Parameters for 100 MW$_e$ falling particle receiver.

Parameter	Value	Basis
Tower height (m):	258	Calculated in SAM [84]
Cavity aperture height (m):	26	Calculated in SAM [84]
Cavity aperture width (m):	28	Calculated in SAM [84]
Receiver elevator height (m):	30	Based on calculated receiver height
Number of recirculation lifts:	1	Two passes (1 lift)
Power plant net output (MW$_e$):	100	Baseline [1]
Power plant thermal-to-electric efficiency:	0.5	Assumed based on higher temperature output and SunShot power cycle target
Parasitic power consumption in power cycle (MW$_e$):	20	Calculated in SAM [84]
Power-cycle design thermal input power (MW$_t$):	220	Calculated in SAM [84]
Solar multiple:	2.09	Baseline [1]
Receiver design thermal power (MW$_t$):	460	Calculated in SAM [84]
Average particle specific heat (J/kg K):	1200	From [18] based on 873 K
Average increase in particle temperature (K):	400	Applicable for supercritical steam or combined supercritical CO_2 power cycles
Hours of storage:	9	Baseline [1]
Price conversion factor from 1982$ to 2016$:	2.46	[85]

sinter at high temperatures and pressures [82]. These types of particles may be suitable for indirect particle heating in tubes where the solar absorptance is not important.

4. Cost estimate

The costs associated with the receiver component of a 100 MW_e high-temperature falling-particle receiver system with 9 h of thermal storage are estimated in this section. For a 100 MW_e plant, the parameter values in Table 4 are used to calculate costs associated with components specific to the falling particle cavity receiver. The System Advisor Model [83] was used to determine some parameters such as tower height, aperture size, and required thermal input power, which impact costs.

Costs for some components specific to the falling particle receiver are estimated using formulas and costs reported in [7]. The cost of the particle elevator as a function of tower height and receiver design thermal power is expressed as follows:

$$Cost_{elevator}\ (\$1982) = THT\left(500 + 27(Q)^{0.292}\right) \quad (1)$$

where THT is the tower height (m) and Q is the receiver design thermal power (kW_t) as described in Table 4. The tower elevator lifts the particles from the base of the tower back to the top of the tower, while the receiver elevator is used to control the mass flow and distribution of the particles entering the receiver. While Olds-type elevators that have been used in prototypical tests have low lift efficiencies (<10%) due to the friction of the particles on the rotating casing, commercial-scale skip hoists (e.g., Kimberly Skip) have lift efficiencies exceeding 80%. The parasitic cost of the particle lift is expected to be comparable to costs for pumping of conventional fluids (water, molten salt). The mass flow rate of particles, $\dot{m}$ (kg/s), can be calculated using the following equation:

$$Q = \dot{m} c_p \Delta T \quad (2)$$

The calculated costs for the tower and receiver elevators, particle-to-fluid heat exchanger, and particles are shown in Table 5 with inflation from 1982 to current (2016) dollars [85]. The cost of ceramic particles, which have been shown to be very durable with no sintering at operating temperatures and pressures expected in a

Table 7
Particle storage system component costs.

Storage system component	Cost ($/kW h_t)	Basis
Tanks	$6.00	[1]
Foundations	$0.70	[1]
Particle media	$9.08	Table 5
Piping/valves	$1.00	[1]
Controls and instrumentation	$0.50	[1]
Spare parts and other directs	$1.00	[1]
Contingency	$4.00	[1]
Total capital cost	$22.28	[1]

Table 5
Calculated costs of falling particle receiver components.

Parameter	Cost	Basis
Tower elevator cost ($) in 1982$	$442656.01	Eq. (1)
Tower elevator cost ($) in 2016$	$1088933.78	[85]
Tower elevator cost/kW_t absorbed ($/$kW_t$)	$2.37	Based on receiver design thermal power (Table 4)
Recirculating elevator cost ($) in 1982$	$51471.63	Eq. (1)
Recirculating elevator cost ($) in 2016$	$126620.21	[85]
Recirculating elevator cost/kW_t absorbed ($/$kW_t$):	$0.28	Based on receiver design thermal power (Table 4)
Total elevator cost ($/$kW_t$):	$2.64	Sum of tower and recirculating elevator costs
Particle-to-fluid heat exchanger ($/$MW_t$) in 1982$:	$20000.00	[7]
Particle-to-fluid heat exchanger ($/$MW_t$) in 2016$:	$49200.00	[85]
Particle-to-fluid heat exchanger ($/$kW_t$) in 2016$:	$49.20	Divide by 1000
Particle-to-fluid heat exchanger ($/$kW_e$) in 2016$:	$98.40	Uses thermal-to-electric efficiency in Table 4
Particle mass flow rate through receiver (kg/s):	958	Eq. (2) where Q is receiver design thermal power (Table 4)
Particle mass flow rate through heat exchanger (kg/s):	458	Eq. (2) where Q is power-cycle design thermal input power (Table 4)
Particle mass flow rate to be lifted (ton/h):	1800	Unit conversion of line above
Mass of particles required (kg):	1.63E+07	556 kg/s × 3600 s/h × 9 h × 1.1 (10% extra)
Mass of particles (tons):	1.8E+04	Unit conversion
Cost of ceramic particles ($/lb):	$0.50	Quote from CARBO Ceramics for bulk pricing
Cost of particles ($/kg) in 2011$:	$1.10	Unit conversion
Cost of particle ($) in 2011$:	$18,000,000	$/kg × mass
Cost of particles ($/kW h_t):	$9.10	Cost of particles divided by (220 × 10^3 kW_t × 9 h). This cost is part of the thermal storage cost

Table 6
Particle receiver component costs ($/$kW_t$).

Receiver component	Cost ($/$kW_t$)	Basis
Receiver	$44.91	Based on scaling from 1 MW prototype receiver costs of structure, hoppers, ducting, insulation [44]
Tower	$57.07	Calculated in SAM [84]; tower cost divided by receiver thermal design power (Table 4)
Particle elevators	$2.64	From Table 5
Controls and instruments	$1.00	Assumed to be the same as baseline external receiver from utility study in [1]
Spare parts and other directs	$1.00	Assumed to be the same as baseline external receiver from utility study in [1]
Contingency	$18.00	Assumed to be the same as baseline external receiver from utility study in [1]
Total receiver cost	$125	

Table 8
Comparison of energy storage technologies.

Metric	Energy storage technology						References
	Solid particles	Molten salt	Batteries	Pumped hydro	Compressed air	Flywheels	
Levelized cost[a] ($/MW h_e)	10–13	11–17	100–1000	150–220	120–210	350–400	[1,87,88]
Round-trip efficiency[b]	>98%	>98%	60–90%	65–80%	40–70%	80–90%	[89–92]
Cycle life	>10,000	>10,000	1000–5000	>10,000	>10,000	>10,000	[90]
Toxicity/environmental impacts	N/A	Reactive with piping materials	Heavy metals pose environmental and health concerns	Water evaporation/consumption	N/A	N/A	
Restrictions/limitations	Particle/fluid heat transfer can be challenging	<600 °C (decomposes above ~600 °C)	Very expensive for utility-scale storage	Large amounts of water required	Unique geography required	Only provides seconds to minutes of storage	

[a] For solid particles and molten salt, we assume a 30–50% thermal-to-electric conversion efficiency and 10,000 lifetime cycles for the thermal-to-electric storage and conversion systems; the cost includes the storage media (bulk ceramic particles and sodium/potassium nitrate salts ~$1/kg with ΔT = 400 °C and 9 h of storage), tanks, pumps/piping/valves, other parts and contingency, and the power block at $1000/$kW_e$ with 19 operating hours per daily cycle (including 9 h of storage) and 90% availability. For batteries, cost is based on sodium-sulfur, vanadium-redox, zinc-bromine, lead-acid, and lithium-ion batteries capable of providing large-scale electricity.
[b] Roundtrip efficiency defined as ratio of energy into energy retrieved from storage.

particle receiver, is ~$1/kg. Silica-based particles (sand) are considerably cheaper. The cost of the particles in $/kW h_t can be determined using the following equation:

$$\$/\text{kW h}_t = \frac{(\$/\text{kg})}{c_p \Delta T}(1000\ \text{W/kW})(3600\ \text{s/h})(1 + inv) \quad (3)$$

where *inv* is an additional fraction of total particle inventory (assumed to be 0.1 or 10%) required to operate the system at full capacity while charging the storage.

Table 6 summarizes the primary component costs of the particle receiver, including hoppers, ducting, insulation, the tower, elevators, controls, spare parts, and contingency. The total estimated cost for a 100 MW_e falling particle receiver is ~$125/$kW_t$, which is less than the Department of Energy SunShot target of $150/$kW_t$ [86].

Table 7 summarizes the estimated cost of the particle storage system, using the particle costs from Table 5. The cost of the tanks, foundation, piping/valves, controls, and other associated costs is taken from those of equivalent components for a molten-salt power tower plant, but the cost of the tanks is expected to be less due to the use of cheaper materials (e.g., firebrick, reinforced concrete). It should be noted that additional studies of particle storage tanks utilizing layers of insulated firebrick, perlite, and refinforced concrete can yield costs that are less than $15/$kW_{hth}$.

The levelized cost of the particle storage and thermal-to-electric conversion system compared to other energy storage technologies is shown in Table 8, along with other comparison metrics. The cost of the power block for thermal storage systems is assumed to be $1000/$kW_e$, and the power block is assumed to operate an average of 10 h during the day plus 9 h at night from storage with an overall availability of 90%. The levelized costs of the thermal storage and conversion systems are at least an order of magnitude less than that of batteries and the other energy storage technologies such as pumped hydro, compressed air energy storage, and flywheels. In addition, pumped hydro and compressed air energy storage requires unique resource and geographic requirements. Flywheels are only applicable for very short-term storage applications. For longer-term, utility-scale energy storage, thermal storage using particles or molten salt is more cost-effective than other currently available technologies.

5. Summary

Particle receivers enable temperatures significantly higher than conventional receivers employing molten nitrate salts, which are limited to less than ~600 °C. Direct particle receivers include free-falling, obstructed-flow, centrifugal, and fluidized designs that irradiate the particles directly. Advantages include the potential for high efficiencies due to direct irradiance of the heat transfer media. Challenges include maintaining and controlling sufficient mass flow and reducing particle loss. Indirect particle receivers include gravity-driven flow in enclosures and fluidized flow in tubes. Advantages include complete containment of the particles, while challenges include additional heat-transfer resistance between the irradiated surfaces and particles. A cost estimate of a 100 MW_e particle receiver was presented. The cost of the particles was estimated to be ~$9/kW h_t for a particle temperature rise of 400 °C, a specific heat of 1200 J/kg K, and 9 h of storage, while the cost of the receiver (including the structure, hoppers, ducting, and insulation) was estimated to be ~$125/$kW_t$. The levelized cost of thermal storage and electricity conversion using particles was estimated to be ~$10/MW h_e, at least an order of magnitude lower than other utility-scale energy storage technologies, including batteries, pumped hydro, and compressed air energy storage.

Acknowledgements

This paper is based upon work supported in part by the DOE SunShot Program (Award DE-EE0000595-1558) and the US-India Partnership to Advance Clean Energy-Research (PACE-R) for the Solar Energy Research Institute for India and the United States (SERIIUS), funded jointly by the U.S. Department of Energy (Office of Science, Office of Basic Energy Sciences, and Energy Efficiency and Renewable Energy, Solar Energy Technology Program, under Subcontract DE-AC36-08GO28308 to the National Renewable Energy Laboratory, Golden, Colorado) and the Government of India, through the Department of Science and Technology under Subcontract IUSSTF/JCERDC-SERIIUS/2012 dated 22nd November 2012. Sandia National Laboratories is a multi-program laboratory managed and operated by Sandia Corporation, a wholly owned subsidiary of Lockheed Martin Corporation, for the U.S. Department of Energy's National Nuclear Security Administration under contract DE-AC04-94AL85000.

References

[1] G.J. Kolb, C.K. Ho, T.R. Mancini, J.A. Gary, Power Tower Technology Roadmap and Cost Reduction Plan SAND2011-2419, Sandia National Laboratories, Albuquerque, NM, 2011.
[2] R.W. Bradshaw, R.W. Carling, A review of the chemical and physical-properties of molten alkali nitrate salts and their effect on materials for solar central receivers, J. Electrochem. Soc. 134 (1987) C510–C511.
[3] E.S. Freeman, The kinetics of the thermal decomposition of sodium nitrate and of the reaction between sodium nitrite and oxygen, J. Phys. Chem. 60 (1956) 1487–1493.
[4] C.K. Ho, B.D. Iverson, Review of high-temperature central receiver designs for concentrating solar power, Renew. Sustain. Energy Rev. 29 (2014) 835–846.
[5] P.K. Falcone, A Handbook for Solar Central Receiver Design SAND86-8009, Sandia National Laboratories, Livermore, CA, 1986.
[6] J.M. Christian, C.K. Ho, Alternative Designs of a High Efficiency, North-Facing, Solid Particle Receiver, SolarPACES 2013, September 17–20, 2013, Las Vegas, NV.
[7] P.K. Falcone, J.E. Noring, J.M. Hruby, Assessment of a Solid Particle Receiver for a High Temperature Solar Central Receiver System SAND85-8208, Sandia National Laboratories, Livermore, CA, 1985.
[8] B. Gobereit, L. Amsbeck, R. Buck, R. Pitz-Paal, H. Müller-Steinhagen, Assessment of a Falling Solid Particle Receiver with Numerical Simulation, SolarPACES 2012, September 11–14, 2012, Marrakech, Morrocco.
[9] C. Ho, J. Christian, D. Gill, A. Moya, S. Jeter, S. Abdel-Khalik, D. Sadowski, N. Siegel, H. Al-Ansary, L. Amsbeck, B. Gobereit, R. Buck, Technology advancements for next generation falling particle receivers, in: Proceedings of the Solarpaces 2013 International Conference, vol. 49, 2014, pp. 398–407.
[10] J.M. Hruby, B.R. Steele, A solid particle central receiver for solar-energy, Chem. Eng. Prog. 82 (1986) 44–47.
[11] S.S.S. Khalsa, J.M. Christian, G.J. Kolb, M. Röger, L. Amsbeck, C.K. Ho, N.P. Siegel, A.C. Moya, CFD simulation and performance analysis of alternative designs for high-temperature solid particle receivers, August 7–10, 2011 ed., ASME International Conference on Energy Sustainability, Washington, DC, USA, 2011.
[12] S.S.S. Khalsa, C.K. Ho, Radiation boundary conditions for computational fluid dynamics models of high-temperature cavity receivers, J Solar Energy Eng-Trans ASME (2011) 133.
[13] K. Kim, S.F. Moujaes, G.J. Kolb, Experimental and simulation study on wind affecting particle flow in a solar receiver, Sol. Energy 84 (2010) 263–270.
[14] G.J. Kolb, R.B. Diver, N. Siegel, Central-station solar hydrogen power plant, J. Solar Energy Eng.-Trans. ASME 129 (2007) 179–183.
[15] Z.W. Ma, G. Glatzmaier, M. Mehos, Fluidized bed technology for concentrating solar power with thermal energy storage, J Solar Energy Eng-Trans ASME (2014) 136.
[16] M.J. Rightley, L.K. Matthews, G.P. Mulholland, Experimental characterization of the heat-transfer in a free-falling-particle receiver, Sol. Energy 48 (1992) 363–374.
[17] M. Röger, L. Amsbeck, B. Gobereit, R. Buck, Face-down solid particle receiver using recirculation, J. Sol.Energy Eng. (2011).
[18] N.P. Siegel, C.K. Ho, S.S. Khalsa, G.J. Kolb, Development and evaluation of a prototype solid particle receiver: on-sun testing and model validation, J. Solar Energy Eng.-Trans. ASME (2010) 132.
[19] T.D. Tan, Y.T. Chen, Review of study on solid particle solar receivers, Renew. Sustain. Energy Rev. 14 (2010) 265–276.
[20] W. Wu, D. Trebing, L. Amsbeck, R. Buck, R. Pitz-Paal, Prototype testing of a centrifugal particle receiver for high-temperature concentrating solar applications, J. Solar Energy Eng.-Trans. ASME (2015) 137.
[21] W. Wu, R. Uhlig, R. Buck, R. Pitz-Paal, Numerical simulation of a centrifugal particle receiver for high-temperature concentrating solar applications, Numer. Heat Transfer Part A – Appl. 68 (2015) 133–149.
[22] G. Flamant, Theoretical and experimental-study of radiant-heat transfer in a solar fluidized-bed receiver, AIChE J. 28 (1982) 529–535.
[23] G. Flamant, D. Hernandez, C. Bonet, J.P. Traverse, Experimental aspects of the thermochemical conversion of solar-energy – decarbonation of $CaCo_3$, Sol. Energy 24 (1980) 385–395.
[24] C.K. Ho, J.M. Christian, J. Yellowhair, K. Armijo, S. Jeter, 2016. Performance Evaluation of a high-temperature falling particle receiver. ASME Power & Energy Conference, June 26–30, 2016, Charlotte, NC.
[25] C.K. Ho, J.M. Christian, J. Yellowhair, N. Siegel, S. Jeter, M. Golob, S.I. Abdel-Khalik, C. Nguyen, H. Al-Ansary, 2015, On sun testing of an advanced falling particle receiver system, SolarPACES 2015, October 13–16, 2015, Cape Town, South Africa.
[26] W. Wu, L. Amsbeck, R. Buck, R. Uhlig, R. Ritz-Paal, Proof of concept test of a centrifugal particle receiver, Proceedings of the Solarpaces 2013 International Conference, vol. 49, 2014, pp. 560–568.
[27] W. Wu, L. Amsbeck, R. Buck, N. Waibel, P. Langner, R. Pitz-Paal, On the influence of rotation on thermal convection in a rotating cavity for solar receiver applications, Appl. Therm. Eng. 70 (2014) 694–704.
[28] G. Flamant, D. Gauthier, H. Benoit, J.L. Sans, B. Boissiere, R. Ansart, M. Hemati, A new heat transfer fluid for concentrating solar systems: particle flow in tubes, Proceedings of the Solarpaces 2013 International Conference, vol. 49, 2014, pp. 617–626.
[29] G. Flamant, D. Gauthier, H. Benoit, J.L. Sans, R. Garcia, B. Boissiere, R. Ansart, M. Hemati, Dense suspension of solid particles as a new heat transfer fluid for concentrated solar thermal plants: on-sun proof of concept, Chem. Eng. Sci. 102 (2013) 567–576.
[30] J. Martinek, Z. Ma, Granular flow and heat-transfer study in a near-blackbody enclosed particle receiver, J. Sol.Energy Eng. 137 (2015). 051008-051008.
[31] A. Steinfeld, A. Imhof, D. Mischler, Experimental investigation of an atmospheric-open cyclone solar reactor for solid-gas thermochemical reactions, J Solar Energy Eng.-Trans. ASME 114 (1992) 171–174.
[32] M. Röger, L. Amsbeck, B. Gobereit, R. Buck, Face-down solid particle receiver using recirculation, J. Solar Energy Eng.-Trans. ASME (2011).
[33] C.K. Ho, J. Christian, D. Romano, J. Yellowhair, N. Siegel. Characterization of particle flow in a free-falling solar particle receiver, in: Proceedings of the ASME 2015 Power and Energy Conversion Conference, June 28–July 2, 2015, San Diego, CA.
[34] J.M. Hruby, B.R. Steele, V.P. Burolla, Solid Particle Receiver Experiments: Radiant Heat Test SAND84-8251, Sandia National Laboratories, Albuquerque, NM, 1984.
[35] J.M. Hruby, A Technical Feasibility Study of a Solid Particle Solar Central Receiver for High Temperature Applications SAND86-8211, Sandia National Laboratories, Livermore, CA, 1986.
[36] G. Evans, W. Houf, R. Greif, C. Crowe, Gas-particle flow within a high-temperature solar cavity receiver including radiation heat-transfer, J. Solar Energy Eng.-Trans. ASME 109 (1987) 134–142.
[37] A. Meier, A predictive CFD model for a falling particle receiver reactor exposed to concentrated sunlight, Chem. Eng. Sci. 54 (1999) 2899–2905.
[38] H. Chen, Y. Chen, H.T. Hsieh, N. Siegel, 2007, CFD modeling of gas particle flow within a solid particle solar receiver, in: Proceedings of the ASME International Solar Energy Conference, pp. 37–48.
[39] H.H. Klein, J. Karni, R. Ben-Zvi, R. Bertocchi, Heat transfer in a directly irradiated solar receiver/reactor for solid-gas reactions, Sol. Energy 81 (2007) 1227–1239.
[40] J. Martin, J. John Vitko, ASCUAS: A Solar Central Receiver Utilizing a Solid Thermal Carrier SAND82-8203, Sandia National Laboratories, Livermore, CA, 1982.
[41] S.S. Khalsa, J.M. Christian, G.J. Kolb, M. Roger, L. Amsbeck, C.K. Ho, N.P. Siegel, A.C. Moya, 2011, CFD simulation and performance analysis of alternative designs for high-temperature solid particle receivers, in: Proceedings of the ASME 2011 Energy Sustainability and Fuel Cell Conference, August 7–10, 2011, Washington D.C.
[42] B. Gobereit, L. Amsbeck, R. Buck, Operation strategies for falling particle receivers, in: Proceedings of ASME 2013 7th International Conference on Energy Sustainability, July 14–19, 2013, Minneapolis, MN.
[43] C.K. Ho, J.M. Christian, Evaluation of air recirculation for falling particle receivers, in: Proceedings of ASME 2013 7th International Conference on Energy Sustainability, July 14–19, 2013, Minneapolis, MN.
[44] J.M. Christian, C.K. Ho, System design of a 1 MW north-facing, solid particle receiver, in: Proceedings of the Solarpaces 2014 International Conference, 2014.
[45] C.K. Ho, J.M. Christian, A.C. Moya, J. Taylor, D. Ray, J. Kelton, Experimental and numerical studies of air curtains for falling particle receivers, in: Proceedings of ASME 2014 8th International Conference on Energy Sustainability, June 29–July 2, 2014, Minneapolis, MN.
[46] R. Knott, D.L. Sadowski, S.M. Jeter, S.I Abdel-Khalik, H.A. Al-Ansary, A. El-Leathy, High temperature durability of solid particles for use in particle heating concentrator solar power systems, in: Proceedings of the ASME 2014 8th International Conference on Energy Sustainability, June 29–July 2, 2014, Boston, MA.
[47] N. Siegel, M. Gross, C. Ho, T. Phan, J. Yuan, Physical properties of solid particle thermal energy storage media for concentrating solar power applications,

Proceedings of the Solarpaces 2013 International Conference, vol. 49, pp. 1015–1023.
[48] N.P. Siegel, M.D. Gross, R. Coury, The development of direct absorption and storage media for falling particle solar central receivers, ASME J. Solar Energy Eng. 137 (2015). 041003-041003-7.
[49] C.K. Ho, S.S. Khalsa, N.P. Siegel, Modeling on-sun tests of a prototype solid particle receiver for concentrating solar power processes and storage, in: ES2009: Proceedings of the ASME 3rd International Conference on Energy Sustainability, vol. 2, San Francisco, CA, pp. 543–550.
[50] G.J. Kolb, Suction-recirculation device for stabilizing particle flows within a solar powered solid particle receiver, U.S. Patent# 8,109,265, 2012.
[51] Z.Q. Chen, Y.T. Chen, T.D. Tan, Numerical analysis on the performance of the solid solar particle receiver with the influence of aerowindow, in: Proceedings of the ASME Fluids Engineering Division Summer Conference, 2008, vol. 1, Pt a and B, Jacksonville, FL, pp. 159–166.
[52] T.D. Tan, Y.T. Chen, Protection of an aerowindow, one scheme to enhance the cavity efficiency of a solid particle solar receiver, in: HT2009: Proceedings of the Asme Summer Heat Transfer Conference 2009, vol. 2, San Francisco, CA, pp. 611–618.
[53] T.D. Tan, Y.T. Chen, Z.Q. Chen, N. Siegel, G.J. Kolb, Wind effect on the performance of solid particle solar receivers with and without the protection of an aerowindow, Sol. Energy 83 (2009) 1815–1827.
[54] T. Lee, S. Lim, S. Shin, D.L. Sadowski, S.I. Abdel-Khalik, S.M. Jeter, H. Al-Ansary, Numerical simulation of particulate flow in interconnected porous media for central particle-heating receiver applications, Sol. Energy 113 (2015) 14–24.
[55] A.W. Khayyat, R.C. Knott, C.L. Nguyen, M.C. Golob, S.I. Abdel-Khalik, S.M. Jeter, H.A. Al-Ansary, Measurement of particulate flow in discrete structure particle heating receivers, in: Proceedings of the ASME 2015 Power and Energy Conversion Conference, June 28–July 2, 2015, San Diego, CA.
[56] G. Xiao, K.K. Guo, M.J. Ni, Z.Y. Luo, K.F. Cen, Optical and thermal performance of a high-temperature spiral solar particle receiver, Sol. Energy 109 (2014) 200–213.
[57] I. Ermanoski, N.P. Siegel, E.B. Stechel, A new reactor concept for efficient solar-thermochemical fuel production, J. Solar Energy Eng.-Trans. ASME (2013) 135.
[58] I. Ermanoski, Maximizing efficiency in two-step solar-thermochemical fuel production, International Conference on Concentrating Solar Power and Chemical Energy Systems, Solarpaces 2014 69 (2015) 1731–1740.
[59] I. Ermanoski, N. Siegel, Annual average efficiency of a solar-thermochemical reactor, Proceedings of the Solarpaces 2013 International Conference, vol. 49, 2014, pp. 1932–1939.
[60] F. Bai, Y. Zhang, X. Zhang, F. Wang, Y. Wang, Z. Wang, Thermal performance of a quartz tube solid particle air receiver, Proceedings of the Solarpaces 2013 International Conference, vol. 49, 2014, pp. 284–294.
[61] F. Wang, F. Bai, Z. Wang, X. Zhang, Numerical simulation of quartz tube solid particle air receiver, International Conference on Concentrating Solar Power and Chemical Energy Systems, Solarpaces 2014 69 (2015) 573–582.
[62] Y.N. Zhang, F.W. Bai, X.L. Zhang, F.Z. Wang, Z.F. Wang, Experimental study of a single quartz tube solid particle air receiver, International Conference on Concentrating Solar Power and Chemical Energy Systems, Solarpaces 2014 69 (2015) 600–607.
[63] M. Abdelrahman, P. Fumeaux, P. Suter, Study of solid-gas-suspensions used for direct absorption of concentrated solar-radiation, Sol. Energy 22 (1979) 45–48.
[64] A.J. Hunt, A new solar receiver utilizing a small particle heat exchanger, in: Proceedings of the 14th International Society of Energy Conversion Engineering Conference, Institute of Electrical and Electronics Engineers, New York, 1979, pp. 159–163.
[65] A.J. Hunt, C.T. Brown, Solar testing of the small particle heat exchanger (SPHER), Report no. LBL-16497, Lawrence Berkeley National Laboratory, Berkeley, CA, 1982.
[66] F. Miller, R. Koenigsdorff, Theoretical-analysis of a high-temperature small-particle solar receiver, Solar Energy Mater. 24 (1991) 210–221.
[67] F.J. Miller, R.W. Koenigsdorff, Thermal modeling of a small-particle solar central receiver, J. Solar Energy Eng.-Trans. ASME 122 (2000) 23–29.
[68] A. Crockerand, F. Miller, Coupled fluid flow and radiation modeling of a cylindrical small particle solar receiver, in: Proceedings of the ASME 6th International Conference on Energy Sustainability, 2012, Pts a and B, pp. 405–412.
[69] P.F. del Campo, F. Miller, A. Crocker, Three-dimensional fluid dynamics and radiative heat transfer modeling of a small particle solar receiver, in: Proceedings of the ASME 7th International Conference on Energy Sustainability, 2014. 2013.
[70] P. Fernandez, F.J. Miller, Performance analysis and preliminary design optimization of a Small Particle Heat Exchange Receiver for solar tower power plants, Sol. Energy 112 (2015) 458–468.
[71] K. Kitzmiller, F. Miller, Thermodynamic cycles for a small particle heat exchange receiver used in concentrating solar power plants, J. Solar Energy Eng.-Trans. ASME (2011) 133.
[72] Z. Ma, R. Zhang, Solid particle thermal energy storage design for a fluidized-bed concentrating solar power plant, 2013.
[73] H. Benoit, I.P. Lopez, D. Gauthier, J.L. Sans, G. Flamant, On-sun demonstration of a 750 degrees C heat transfer fluid for concentrating solar systems: dense particle suspension in tube, Sol. Energy 118 (2015) 622–633.
[74] H.J. Chen, Y.T. Chen, H.T. Hsieh, G. Kolb, N. Siegel, Numerical investigation on optimal design of solid particle solar receiver, Proc. Energy Sustain. Conf. 2007 (2007) 971–979.
[75] H.J. Chen, Y.T. Chen, H.T. Hsieh, N. Siegel, Computational fluid dynamics modeling of gas-particle flow within a solid-particle solar receiver, J. Solar Energy Eng.-Trans. ASME 129 (2007) 160–170.
[76] C.K. Ho, M. Roeger, S.S. Khalsa, L. Amsbeck, R. Buck, N. Siegel, G. Kolb, Experimental validation of different modeling approaches for solid particle receivers, SolarPACES 2009, September 15–18, 2009, Berlin, Germany.
[77] N. Siegel, G. Kolb, K. Kim, V. Rangaswamy, S. Moujaes, Solid particle receiver flow characterization studies, Proc. Energy Sustain. Conf. 2007 (2007) 877–883.
[78] H.e.a. Al Ansary, Solid particle receiver with porous structure for flow regulation and enhancement of heat transfer, 2013.
[79] B. Hoffschmidt, F.M. Tellez, A. Valverde, J. Fernandez, V. Fernandez, Performance evaluation of the 200-kW(th) HiTRec-II open volumetric air receiver, J. Solar Energy Eng.-Trans. ASME 125 (2003) 87–94.
[80] International, R., 1983, Final Report Sodium Solar Receiver Experiment, SAND82-8192, December 1983, Sandia National Laboratories.
[81] H. Al-Ansary et al., Characterization and sintering potential of solid particles for use in high temperature thermal energy storage system, SolarPACES 2013, September 17–20, 2013, Las Vegas, NV.
[82] R. Knott, D.L. Sadowski, S.M. Jeter, S.I. Abdel-Khalik, H.A. Al-Ansary, A. El-Leathy, Sintering of solid particulates under elevated temperature and pressure in large storage bins for thermal energy storage, Proceedings of the ASME 2014 8th International Conference on Energy Sustainability, June 29–July 2, 2014, Boston, MA.
[83] System Advisor Model, 2012 <https://sam.nrel.gov/>.
[84] National Renewable Energy Laboratory <https://sam.nrel.gov>.
[85] From http://www.bls.gov/data/inflation_calculator.htm.
[86] SunShot Vision Study, 2012, from <http://www1.eere.energy.gov/solar/sunshot/vision_study.html>.
[87] H.M. Branz, W. Regan, K.J. Gerst, J.B. Borak, E.A. Santori, Hybrid solar converters for maximum exergy and inexpensive dispatchable electricity, Energy Environ. Sci. 8 (2015) 3083–3091.
[88] A.A. Akhil, DOE/EPRI Electricity Storage Handbook in Collaboration with NRECA SAND2015-1002, Sandia National Laboratories, Albuquerque, NM, 2015.
[89] E. Djajadiwinata, H. Al-Ansary, S. Danish, A. El-Leathy, Z. Al-Suhaibani, Modeling of transient energy loss from a cylindrical-shaped solid particle thermal energy storage tank for central receiver applications, in: Proceedings of the Asme 8th International Conference on Energy Sustainability, 2014, vol. 1.
[90] N.P. Siegel, Thermal energy storage for solar power production, Wiley Interdiscipl. Rev.-Energy Environ. 1 (2012) 119–131.
[91] Energy Storage Technologies, 2016 <http://energystorage.org/energy-storage/energy-storage-technologies>.
[92] Round Trip Efficiency, 2016, from <https://energymag.net/round-trip-efficiency/>.